VERSITA

Central European Journal of Chemistry
DOI: 10.2478/s11532-007-0012-1
Research article
CEJC 5(2) 2007 396–419

A theoretical investigation on the isomerism and the NMR properties of thiosemicarbazones

N.W.S.V. Nuwan De Silva, Titus V. Albu*

Department of Chemistry,
Tennessee Technological University,
Cookeville, Tennessee 38505, USA

Received 8 November 2006; accepted 28 December 2006

Abstract: Hybrid density functional theory calculations at the mPW1PW91/6-31+G(d,p) level of theory have been used to investigate the optimized structures and other molecular properties of five different series of thiosemicarbazones. The investigated compounds were obtained from acenaphthenequinone, isatin and its derivatives, and alloxan. The focus of the study is the isomerism and the NMR characterization of these thiosemicarbazones. It was found that only one isomer is expected for thiosemicarbazones and methylthiosemicarbazones, while for dimethylthiosemicarbazones, two isomers are possible. All investigated thiosemicarbazones exhibit a hydrazinic proton that is highly deshielded and resonates far downfield in the proton NMR spectra. This proton is a part of a characteristic six-membered ring, and its NMR properties are a result of its strong, intermolecular hydrogen bond. The relationships between the calculated ^{1}H and ^{13}C NMR chemical shifts and various geometric parameters are reported.

Keywords: Thiosemicarbazones, isomerism, NMR chemical shifts, hybrid density functional theory

1 Introduction

Transition metal complexes with heterocyclic thiosemicarbazone (TSC) ligands have attracted a great deal of research interest owing to their potential biological activity [1]. TSC ligands have invited considerable interest for a variety of reasons, such as variable bonding properties, because of the presence of several donor sites, structural diversity and pharmacological aspects. As medicinal reagents, TSC metal complexes have been deemed to be crucial in antifungal, antiviral, anticancer and antitumor therapy [2–6].

* E-mail: albu@tntech.edu

It was proposed that TSC drugs may act to inhibit viruses by chelating to copper(II) a constituent of the virus. In particular, certain copper(II) chelate complexes with thiosemicarbazones exhibit a hypoxic selectivity [7] and are used as carriers for radioactive Cu isotope transport to tumor cells [8, 9].

Thiosemicarbazones are typically obtained in condensation reactions between ketones and thiosemicarbazides. The thiosemicarbazones investigated in the current study were obtained starting from α-diketo compounds. The study focuses on five series of thiosemicarbazones based on acenaphthenequinone, isatin, 1-methylisatin, isatin-5-sulfonate, and alloxan. Each series includes the thiosemicarbazone (TSC), the N4′-methylthiosemicarbazone (MTSC), and the N4′-dimethylthiosemicarbazone (DMTSC). In total, fifteen molecules were investigated: acenaphthenequinone TSC (**1**) denoted ANQ-TSC, acenaphthenequinone MTSC (**2**) denoted ANQ-MTSC, acenaphthenequinone DMTSC (**3**) denoted ANQ-DMTSC, isatin-3-thiosemicarbazone (**4**) denoted I-TSC, isatin MTSC (**5**) denoted I-MTSC, isatin DMTSC (**6**) denoted I-DMTSC, 1-methylisatin-3-thiosemicarbazone (**7**) denoted MI-TSC, 1-methylisatin MTSC (**8**) denoted MI-MTSC, 1-methylisatin DMTSC (**9**) denoted MI-DMTSC, isatin-5-sulfonate-3-thiosemicarbazone (**10**) denoted IS-TSC, isatin-5-sulfonate MTSC (**11**) denoted IS-MTSC, isatin-5-sulfonate DMTSC (**12**) denoted IS-DMTSC, alloxan thiosemicarbazone (**13**) denoted ALL-TSC, alloxan MTSC (**14**) denoted ALL-MTSC, and alloxan DMTSC (**15**) denoted ALL-DMTSC [10]. The optimized structures of these compounds are shown in Figures 1-5. The IUPAC numbering scheme of the thiosemicarbazone moiety and the definition of H_A, H_B, and H_C protons are given in Figure 6.

Acenaphthenequinone, a polycyclic aromatic compound derived from naphthalene, is used as an intermediate for the manufacturing of dyes, pharmaceuticals and pesticides. ANQ-TSC, ANQ-MTSC, and ANQ-DMTSC were synthesized and characterized by ^{1}H NMR, ^{13}C NMR and infrared spectroscopy by Lisic and coworkers [11, 12]. Alloxan is an especially interesting diketo compound because it was reported to be a potent agent for the selective destruction of pancreatic β-cells of mice which can result in inducing permanent diabetes [13–15]. ALL-TSC was found to be active in vitro against a wide variety of bacteria, yeasts, and molds that are pathogenic to animals and plants, and it was also used in formulating mold-resistant vinyl coatings and plasticizers [16]. Lisic and coworkers [17] recently reported the synthesis and spectroscopic properties of an alloxan thiosemicarbazone series that includes the three compounds examined here.

Isatin-based thiosemicarbazones have long been investigated for their benefic biological activity [18]. I-TSC and MI-TSC were the first antiviral drugs used in humans [19], and it has been proposed that their mode of action may involve metal ion chelation [20]. MI-TSC as well as 1-ethylisatin and 2-hydroxyethyl thiosemicarbazones were determined to be effective antiviral chemoprophylactic agents in tissue cultures, animal studies, and clinical practice [21]. Different derivatives of MI-TSC also possess significant anticancer activity [22]. It was also found that isatin-based thiosemicarbazones protect mice against intracerebral vaccinia virus while isatin-based semicarbazones were inactive [23].

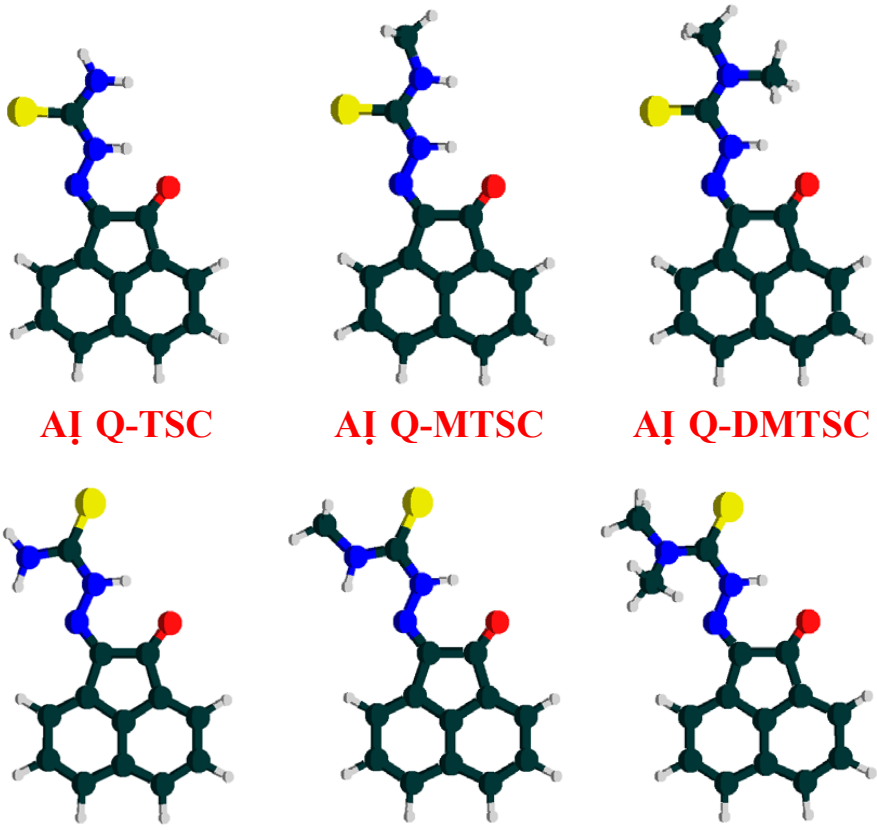

Fig. 1 Optimized structures of acenaphthenequinone-based thiosemicarbazones.

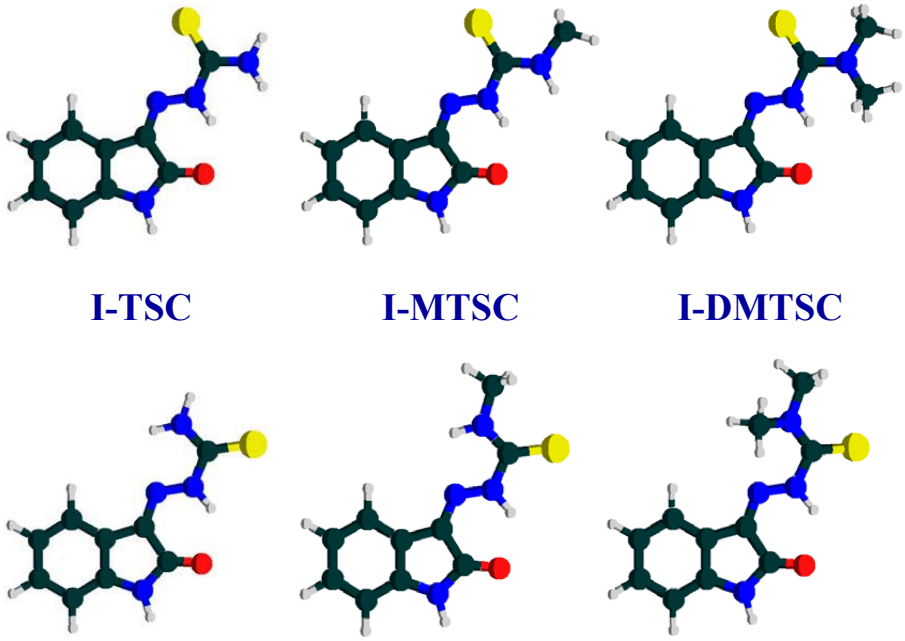

Fig. 2 Optimized structures of isatin-based thiosemicarbazones.

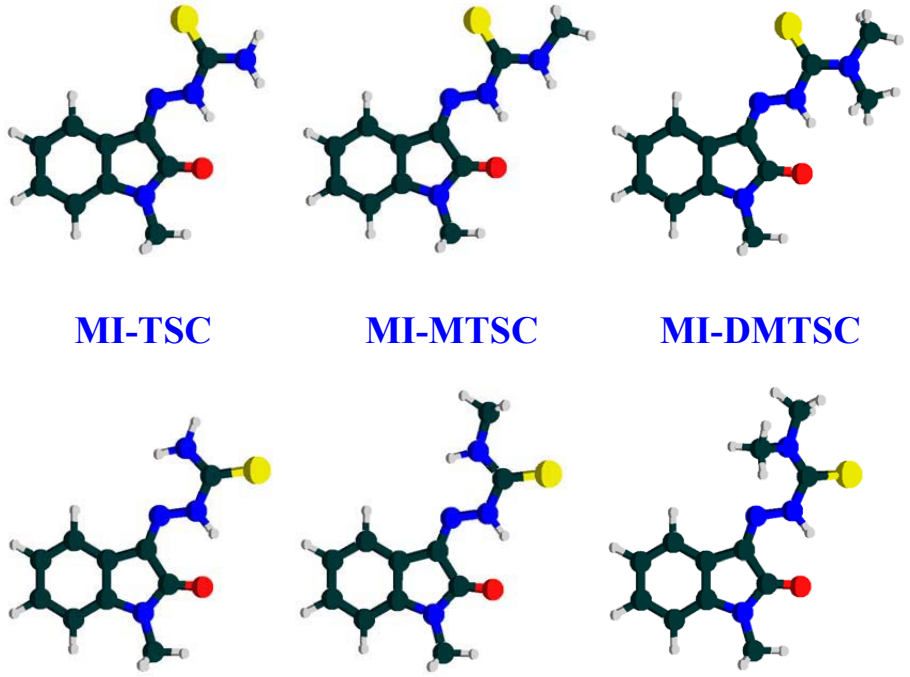

Fig. 3 Optimized structures of 1-methylisatin-based thiosemicarbazones.

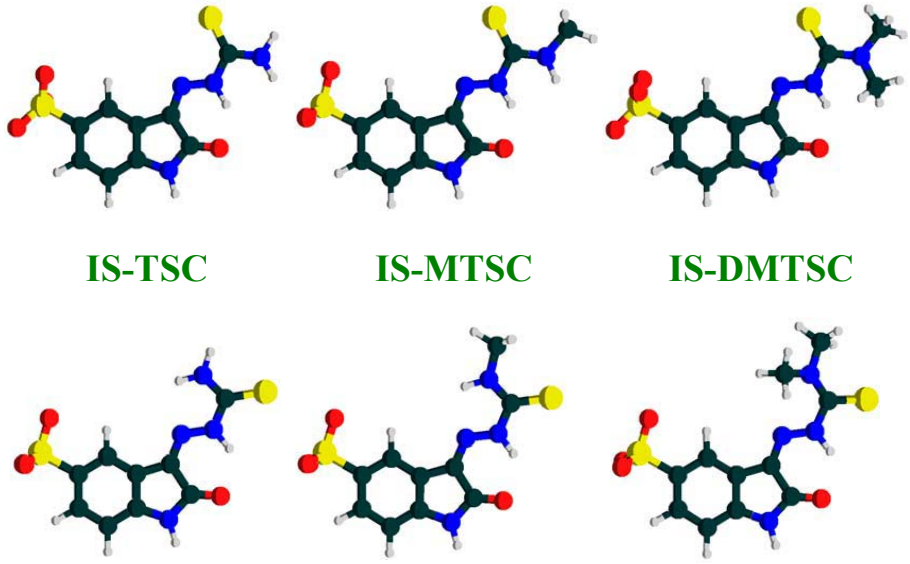

Fig. 4 Optimized structures of isatin-5-sulfonate-based thiosemicarbazones.

Bain et al. [24] reported the synthesis and spectroscopic investigations of N4′-substituted isatin thiosemicarbazones and their copper(II) complexes. MI-MTSC, MI-DMTSC and their complexes with cobalt(II), nickel(II), and copper(II) ions were prepared and characterized by spectral methods [25]. Other derivatives obtained by substituting groups at different other positions of the isatin and TSC moieties were also reported [12, 26–29]. In a few of these studies the focus was on obtaining water-soluble analogues of isatin thiosemicarbazone by substituting isatin at the aromatic ring. Sulfonic acid derivatives

are especially interesting because they are ionized in the sulfonate form in solution. The synthesis and properties of IS-TSC [27], IS-MTSC [12], and IS-DMTSC [12] were reported. A few more recent studies describe the synthesis and structural characterization of transition metal complexes of thiosemicarbazones derived from isatin and its derivatives [30–34].

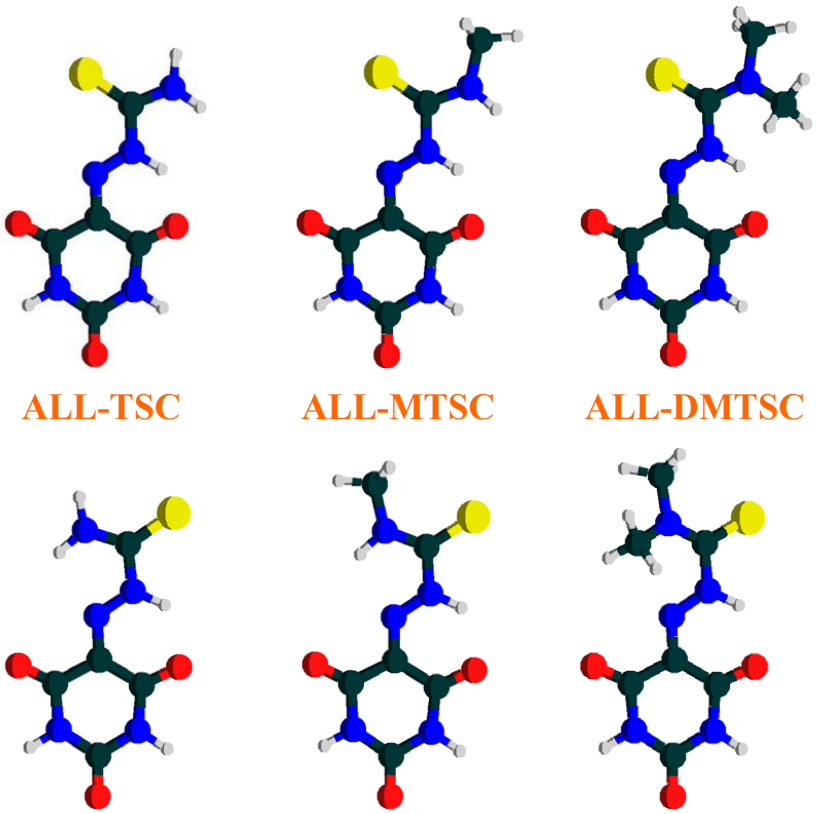

Fig. 5 Optimized structures of alloxan-based thiosemicarbazones.

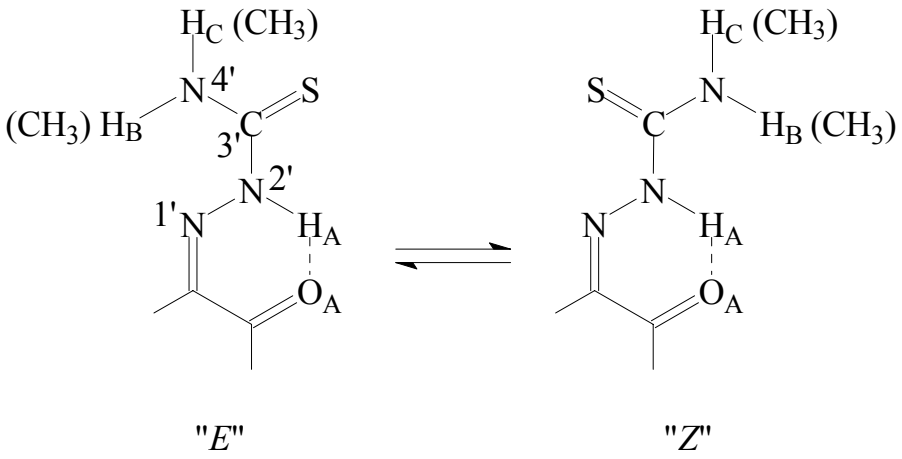

Fig. 6 The equilibrium between the two investigated isomers, the numbering scheme for the thiosemicarbazone moiety, and the definition of other significant atoms.

In an early study of IS-TSC by Stünzi [35], the *Z* and *E* isomers obtained with respect to the C=N1′ bond and the *Z*–*E* isomerization process were investigated in aqueous solution. It was found that the *Z* isomer is favored over the *E* isomer by approximately an order of magnitude. Based on this and other reported experimental results, as presented in Figures 1-5, for the thiosemicarbazones investigated in this study, only the *Z* isomers were considered. Figure 6 shows that only the Z configuration with respect to the C=N1′ bond allow for an intramolecular hydrogen bond interaction between H_A and O_A. More recently, the study of Bain et al. [24] on I-DMTSC and other thiosemicarbazones reported the existence of two isomers obtained by rotation around the N2′–C3′ bond. This is formally a single bond and the two structures should be just conformers, but if the rotation around the N2′–C3′ bond were impeded, the two structures can be considered as geometric isomers. Bain et al. labeled these isomers as *ZE* and *ZZ* isomers to include the *Z* configuration around C=N1′ bond. In the current paper, it is preferred to abandon the first *Z* and to label the two isomers just *E* and *Z*, as presented in Figure 6. The relative distribution between the two isomers was found to be 85:15, however Bain et al. could not distinguish experimentally which of the two observed isomers is more abundant.

Theoretical studies can further advance the understanding of the molecular properties of TSC compounds and their complexes with transitional metals, and a few such studies have been recently reported [36–41]. Some studies have focused on optimized geometries and conformational distribution [37, 38] while others have focused mainly on their NMR properties [39–41]. We recently reported the results of a hybrid density functional theory investigation of a series of alloxan-based thiosemicarbazones and semicarbazones [42]. In a related study, the conformational analysis of 4-methyl-3-thiosemicarbazide was investigated using ab initio methods by Chambers et al. [43].

The hybrid density functional theory study presented here investigates the relative stabilities of various isomers (or conformers) of the investigated thiosemicarbazones and the correlation between the calculated and experimental ^{1}H and ^{13}C NMR chemical shifts. Relationships between the NMR chemical shifts and various molecular parameters are examined. The results can also be used to assign more accurately some ^{1}H and ^{13}C chemical shifts that are experimentally difficult to interpret.

2 Computational Methods

The level of electronic structure theory used in this study is mPW1PW91 [44] in conjunction with the 6-31+G(d,p) basis set. The mPW1PW91 method is a hybrid density functional theory method that employs a 25% Hartree-Fock exchange contribution, the modified Perdew-Wang (mPW) exchange functional [44], and the PW91 correlation functional [45]. This hybrid density functional theory method gives accurate molecular properties such as geometries, vibrational frequencies, and enthalpies of formation, and it was also shown to give accurate NMR chemical shifts [46, 47]. The results obtained in our previous study [42] showed that the methodology employed here is appropriate for studying this class of compounds.

Table 1 Selected distances (A) and angles (degree) in the optimized geometries determined at the mPW1PW91/6-31+G(d,p) level of theory.

Compound	r N2′–H$_A$	r O$_A$···H$_A$	r N2′···O$_A$	θ N2′–H$_A$···O$_A$	θ N1′–N2′–H$_A$	θ C3′–N2′···H$_A$
(**1**) ANQ-TSC (*E*)	1.021	1.986	2.752	129.7	120.8	118.8
(**1**) ANQ-TSC (*Z*)	1.024	1.886	2.720	136.3	117.2	121.4
(**2**) ANQ-MTSC (*E*)	1.021	1.989	2.753	129.5	120.8	118.6
(**2**) ANQ-MTSC (*Z*)	1.025	1.880	2.718	136.6	117.0	121.5
(**3**) ANQ-DMTSC (*E*)	1.021	1.985	2.760	130.5	119.3	116.4
(**3**) ANQ-DMTSC (*Z*)	1.022	1.887	2.723	136.7	116.8	122.0
(**4**) I-TSC (*E*)	1.022	1.982	2.757	130.4	120.6	119.0
(**4**) I-TSC (*Z*)	1.026	1.892	2.732	136.8	117.2	121.4
(**5**) I-MTSC (*E*)	1.022	1.998	2.767	129.9	120.8	118.6
(**5**) I-MTSC (*Z*)	1.026	1.885	2.728	137.2	117.0	121.4
(**6**) I-DMTSC (*E*)	1.023	1.988	2.771	131.2	119.3	116.4
(**6**) I-DMTSC (*Z*)	1.023	1.892	2.733	137.3	116.8	122.0
(**7**) MI-TSC (*E*)	1.022	1.984	2.758	130.4	120.6	119.0
(**7**) MI-TSC (*Z*)	1.026	1.882	2.725	137.1	117.0	121.5
(**8**) MI-MTSC (*E*)	1.022	1.987	2.760	130.2	120.6	118.7
(**8**) MI-MTSC (*Z*)	1.026	1.883	2.727	137.2	116.9	121.5
(**9**) MI-DMTSC (*E*)	1.023	1.986	2.769	131.2	119.2	116.5
(**9**) MI-DMTSC (*Z*)	1.024	1.890	2.732	137.3	116.7	121.9
(**10**) IS-TSC (*E*)	1.021	1.991	2.762	130.2	120.7	119.7
(**10**) IS-TSC (*Z*)	1.027	1.836	2.696	139.0	116.8	121.0
(**11**) IS-MTSC (*E*)	1.020	2.000	2.767	129.9	120.8	119.4
(**11**) IS-MTSC (*Z*)	1.027	1.831	2.695	139.4	116.5	121.1
(**12**) IS-DMTSC (*E*)	1.022	1.993	2.775	131.2	119.4	116.9
(**12**) IS-DMTSC (*Z*)	1.024	1.837	2.699	139.5	116.3	121.7
(**13**) ALL-TSC (*E*)	1.024	1.908	2.652	126.8	121.2	119.3
(**13**) ALL-TSC (*Z*)	1.030	1.773	2.606	135.2	117.0	121.8
(**14**) ALL-MTSC (*E*)	1.024	1.908	2.651	126.8	121.2	119.0
(**14**) ALL-MTSC (*Z*)	1.030	1.769	2.605	135.4	116.9	121.8
(**15**) ALL-DMTSC (*E*)	1.026	1.886	2.650	128.6	119.9	117.0
(**15**) ALL-DMTSC (*Z*)	1.028	1.782	2.611	134.9	117.1	122.0

All investigated systems are closed-shell systems, and the calculations were carried out using restricted wave functions. The sulfonic acid derivatives were calculated in ionized form with a charge of –1; all other systems were neutral. The molecular optimizations were carried out using tight convergence criteria to properly define the molecular geometries. The optimized minimum structures determined to be true energy minima (not

saddle points) by vibrational analysis that yielded no imaginary frequencies. The saddle point optimizations give structures characterized by one imaginary frequency. The NMR chemical shifts were obtained from Gauge-Independent Atomic Orbital (GIAO) calculations [48–50] at the same level of theory, mPW1PW91/6-31+G(d,p), as the geometry optimization. To convert the chemical shifts to ppm and compare them with the experimental values, the calculated isotropic values were subtracted from the calculated isotropic values of ^{1}H and ^{13}C in optimized TMS (31.6515 and 196.597, respectively) at the same level of theory. Atomic charges based on Mulliken population analysis [51–54] and based on generalized atomic polar tensor (GAPT) methodology [55–57] were calculated. All electronic structure calculations were carried out using the Gaussian 03 suite of programs [58].

3 Results

The results of this study are presented in five tables and five figures. Table 1 lists selected optimized geometrical parameters (describing atom locations around H_A) for the studied compounds, and Table 2 lists calculated energetic parameters, relative isomeric populations, and calculated dipole moments. Tables 3 and 4 list selected experimental and calculated ^{1}H NMR and ^{13}C NMR chemical shifts, respectively. Finally, Table 5 lists selected GAPT and Mulliken atomic charges for all investigated compounds.

Table 2 Calculated energetic parameters for the $Z \rightarrow E$ isomerization process (kcal/mol), the calculated relative abundance of the two isomers at 298 K, and the calculated dipole moments (D) for the two isomers.

Compound	ΔE	ΔH_0	ΔH_{298}	ΔG_{298}	N_E/N_Z	μ (E)	μ (Z)
(**1**) ANQ-TSC	-7.37	-6.97	-7.15	-6.57	6.5×10^4	7.66	5.22
(**2**) ANQ-MTSC	-7.50	-7.15	-7.29	-6.83	1.0×10^5	7.32	4.57
(**3**) ANQ-DMTSC	-1.37	-1.11	-1.26	-0.25	1.5	6.81	4.76
(**4**) I-TSC	-7.21	-6.79	-6.99	-6.21	3.6×10^4	7.06	5.22
(**5**) I-MTSC	-7.33	-6.99	-7.12	-6.61	7.0×10^4	6.73	4.74
(**6**) I-DMTSC	-1.26	-0.99	-1.17	0.02	0.97	6.26	5.03
(**7**) MI-TSC	-7.27	-6.87	-7.06	-6.39	4.9×10^4	7.02	5.78
(**8**) MI-MTSC	-7.39	-7.08	-7.20	-6.76	9.0×10^4	6.63	5.26
(**9**) MI-DMTSC	-1.36	-1.23	-1.32	-0.65	3.0	6.11	5.53
(**10**) IS-TSC	-12.03	-11.79	-11.81	-11.91	5.5×10^8	11.39	18.89
(**11**) IS-MTSC	-12.62	-11.99	-12.24	-10.91	1.0×10^8	11.76	20.76
(**12**) IS-DMTSC	-5.90	-5.44	-5.60	-4.54	2.1×10^3	12.64	22.13
(**13**) ALL-TSC	-9.96	-9.30	-9.61	-7.93	6.6×10^5	1.78	5.80
(**14**) ALL-MTSC	-10.11	-9.58	-9.75	-8.66	2.3×10^6	2.16	6.23
(**15**) ALL-DMTSC	-4.15	-3.71	-3.89	-2.92	1.4×10^2	3.34	6.77

Table 3 Experimental and calculated ^{1}H NMR chemical shifts (ppm)

Compound	H_A		H_B, H_C	
	exp[a]	calc[b]	exp	calc
(**1**) ANQ-TSC (*E*)	12.507	13.313	9.312, 8.813	7.385, 5.884
(**1**) ANQ-TSC (*Z*)		14.343		5.121, 5.677
(**2**) ANQ-MTSC (*E*)	12.620	13.339	9.38	7.556
(**2**) ANQ-MTSC (*Z*)		14.417		5.296
(**3**) ANQ-DMTSC (*E*)		13.160		
(**3**) ANQ-DMTSC (*Z*)	13.445	14.186		
(**4**) I-TSC (*E*)	12.46	12.897	9.01, 8.63	7.265, 5.876
(**4**) I-TSC (*Z*)		13.835		5.071, 5.722
(**5**) I-MTSC (*E*)	12.595	12.875	9.24	7.464
(**5**) I-MTSC (*Z*)		13.926		5.248
(**6**) I-DMTSC (*E*)	13.115	12.796		
(**6**) I-DMTSC (*Z*)	13.411	13.714		
(**7**) MI-TSC (*E*)	12.39	12.956	9.05, 8.70	7.237, 5.817
(**7**) MI-TSC (*Z*)		13.966		5.099, 5.683
(**8**) MI-MTSC (*E*)	12.58	12.976	9.328	7.429
(**8**) MI-MTSC (*Z*)		13.883		5.185
(**9**) MI-DMTSC (*E*)		12.846		
(**9**) MI-DMTSC (*Z*)	13.64	13.766		
(**10**) IS-TSC (*E*)	12.466	12.651	8.988, 8.886	7.544, 5.583
(**10**) IS-TSC (*Z*)		14.307		4.671, 5.122
(**11**) IS-MTSC (*E*)	12.544	12.711	9.434	7.744
(**11**) IS-MTSC (*Z*)		14.217		4.889
(**12**) IS-DMTSC (*E*)		12.758		
(**12**) IS-DMTSC (*Z*)	13.348	13.958		
(**13**) ALL-TSC (*E*)	13.406	13.280	9.503, 8.614	7.712, 6.215
(**13**) ALL-TSC (*Z*)		14.747		5.414, 6.129
(**14**) ALL-MTSC (*E*)	13.532	13.347	9.467	7.932
(**14**) ALL-MTSC (*Z*)		14.821		5.588
(**15**) ALL-DMTSC (*E*)		13.522		
(**15**) ALL-DMTSC (*Z*)	14.251	14.600		

[a] The experimental results for ANQ-TSC and ANQ-MTSC are from reference [11], for ANQ-DMTSC, IS-TSC, IS-MTSC, and IS-DMTSC are from reference [12], for I-TSC, I-MTSC, I-DMTSC are from reference [24], for MI-TSC are from reference [33], for MI-MTSC and MI-DMTSC are from reference [25], and for ALL-TSC, ALL-MTSC, and ALL-DMTSC are from reference [17]. All data is obtained in DMSO-d^6.

[b] The calculated results are in gas phase.

Table 4 Experimental and calculated ^{13}C NMR chemical shifts (ppm)[a].

Compound	C{=O$_A$}		C{=N1′}		C3′	
	exp[a]	calc[b]	exp	calc	exp	calc
(**1**) ANQ-TSC (*E*)	189.223	185.094		131.591	179.66	175.546
(**1**) ANQ-TSC (*Z*)		186.456		136.588		176.288
(**2**) ANQ-MTSC (*E*)	189.173	184.461		130.916	178.60	175.013
(**2**) ANQ-MTSC (*Z*)		186.312		135.163		175.501
(**3**) ANQ-DMTSC (*E*)		183.913		131.888		181.135
(**3**) ANQ-DMTSC (*Z*)	180.57	185.830	141.49	136.307	190.13	175.816
(**4**) I-TSC (*E*)	162.68	156.207	132.15	124.688	178.73	175.248
(**4**) I-TSC (*Z*)		157.527		129.851		175.739
(**5**) I-MTSC (*E*)	162.61	156.746	131.55	123.487	177.67	174.965
(**5**) I-MTSC (*Z*)		158.086		128.073		176.272
(**6**) I-DMTSC (*E*)	162.66	155.741		124.249	178.99	180.855
(**6**) I-DMTSC (*Z*)	162.86	157.375	134.74	128.896	182.12	175.804
(**7**) MI-TSC (*E*)	160.7	156.613	131.2	124.800	178.7	175.636
(**7**) MI-TSC (*Z*)		156.897		129.993		175.927
(**8**) MI-MTSC (*E*)	161.0	155.994	143.7	124.132	188.4	174.683
(**8**) MI-MTSC (*Z*)		156.817		128.541		175.761
(**9**) MI-DMTSC (*E*)		155.406		124.628		180.821
(**9**) MI-DMTSC (*Z*)	161.8	156.698	142.8	129.546	180.1	175.848
(**10**) IS-TSC (*E*)	163.630	157.620		129.318	179.634	175.473
(**10**) IS-TSC (*Z*)		159.713		134.673		177.516
(**11**) IS-MTSC (*E*)	163.650	157.441		128.163	178.277	174.963
(**11**) IS-MTSC (*Z*)		158.130		132.329		175.192
(**12**) IS-DMTSC (*E*)		157.503		129.012		180.884
(**12**) IS-DMTSC (*Z*)	163.781	158.978		133.993	179.599	176.479
(**13**) ALL-TSC (*E*)	162.330	155.142		111.997	179.760	175.991
(**13**) ALL-TSC (*Z*)		157.472		117.877		174.011
(**14**) ALL-MTSC (*E*)	162.426	155.334	121.632	111.464	178.139	174.904
(**14**) ALL-MTSC (*Z*)		157.360		117.065		174.068
(**15**) ALL-DMTSC (*E*)		155.440		112.488		178.580
(**15**) ALL-DMTSC (*Z*)	162.891	157.307	150.486	118.054	179.806	175.921

[a] The experimental results for ANQ-TSC and ANQ-MTSC are from reference [11], for ANQ-DMTSC, IS-TSC, IS-MTSC, and IS-DMTSC are from reference [12], for I-TSC, I-MTSC, I-DMTSC are from reference [24], for MI-TSC are from reference [33], for MI-MTSC and MI-DMTSC are from reference [25], and for ALL-TSC, ALL-MTSC, and ALL-DMTSC are from reference [17]. All data is obtained in DMSO-d^6.

[b] The calculated results are in gas phase.

Table 5 Calculated GAPT and Mulliken atomic charges for selected atoms in the investigated thiosemicarbazones.

Compound	H_A		N2′		O_A	
	GAPT	Mulliken	GAPT	Mulliken	GAPT	Mulliken
(**1**) ANQ-TSC (*E*)	0.221	0.383	-1.106	-0.062	-0.656	-0.501
(**1**) ANQ-TSC (*Z*)	0.213	0.349	-1.144	0.102	-0.753	-0.513
(**2**) ANQ-MTSC (*E*)	0.218	0.384	-1.128	-0.145	-0.662	-0.497
(**2**) ANQ-MTSC (*Z*)	0.206	0.345	-1.168	-0.064	-0.747	-0.507
(**3**) ANQ-DMTSC (*E*)	0.209	0.382	-1.106	-0.198	-0.676	-0.489
(**3**) ANQ-DMTSC (*Z*)	0.215	0.352	-1.160	-0.039	-0.736	-0.517
(**4**) I-TSC (*E*)	0.220	0.379	-1.080	-0.091	-0.719	-0.542
(**4**) I-TSC (*Z*)	0.211	0.347	-1.118	0.094	-0.814	-0.566
(**5**) I-MTSC (*E*)	0.217	0.377	-1.100	-0.212	-0.727	-0.541
(**5**) I-MTSC (*Z*)	0.204	0.344	-1.143	-0.010	-0.808	-0.569
(**6**) I-DMTSC (*E*)	0.208	0.377	-1.078	-0.247	-0.740	-0.531
(**6**) I-DMTSC (*Z*)	0.214	0.347	-1.137	-0.002	-0.796	-0.569
(**7**) MI-TSC (*E*)	0.226	0.383	-1.093	-0.080	-0.725	-0.560
(**7**) MI-TSC (*Z*)	0.220	0.350	-1.133	0.092	-0.813	-0.573
(**8**) MI-MTSC (*E*)	0.223	0.383	-1.114	-0.177	-0.730	-0.555
(**8**) MI-MTSC (*Z*)	0.213	0.346	-1.158	-0.013	-0.808	-0.577
(**9**) MI-DMTSC (*E*)	0.214	0.381	-1.091	-0.230	-0.743	-0.542
(**9**) MI-DMTSC (*Z*)	0.222	0.352	-1.150	-0.013	-0.797	-0.580
(**10**) IS-TSC (*E*)	0.219	0.375	-1.122	-0.234	-0.787	-0.560
(**10**) IS-TSC (*Z*)	0.226	0.352	-1.152	0.084	-0.885	-0.584
(**11**) IS-MTSC (*E*)	0.216	0.377	-1.156	-0.214	-0.792	-0.555
(**11**) IS-MTSC (*Z*)	0.216	0.343	-1.191	-0.049	-0.873	-0.585
(**12**) IS-DMTSC (*E*)	0.208	0.376	-1.129	-0.216	-0.802	-0.560
(**12**) IS-DMTSC (*Z*)	0.226	0.351	-1.183	-0.054	-0.873	-0.599
(**13**) ALL-TSC (*E*)	0.251	0.395	-0.861	-0.029	-0.700	-0.528
(**13**) ALL-TSC (*Z*)	0.251	0.369	-0.941	0.107	-0.779	-0.537
(**14**) ALL-MTSC (*E*)	0.249	0.393	-0.860	-0.054	-0.707	-0.521
(**14**) ALL-MTSC (*Z*)	0.246	0.368	-0.945	-0.034	-0.775	-0.543
(**15**) ALL-DMTSC (*E*)	0.243	0.393	-0.838	-0.226	-0.713	-0.506
(**15**) ALL-DMTSC (*Z*)	0.247	0.378	-0.931	-0.049	-0.766	-0.538

Figure 7 presents the plots of calculated ^{1}H NMR chemical shifts versus experimental ^{1}H NMR chemical shifts for H_A. Figures 8-10 show calculated and experimental ^{1}H NMR chemical shifts as a function of particular geometric parameters. Figure 11 shows a representation of the ^{1}H NMR chemical shifts versus the calculated vibrational frequency for the N2′–H_A stretching. In all these figures, the experimental values were taken from the references listed in the appropriate table. A color-labeling scheme was used in Figures 1-5

and 7-11, as follows: acenaphthenequinone series (ANQ) results are in red, isatin series (I) results are in dark blue, 1-methylisatin (MI) results are in blue, isatin-5-sulfonate (IS) series results are in green, and alloxan (ALL) series results are in orange. In Figures 7-11, the TSC results are presented as squares, the MTSC results are presented as circles, the results for the *Z* isomer of DMTSC are presented as diamonds, and the *E* isomer of DMTSC are presented as triangles.

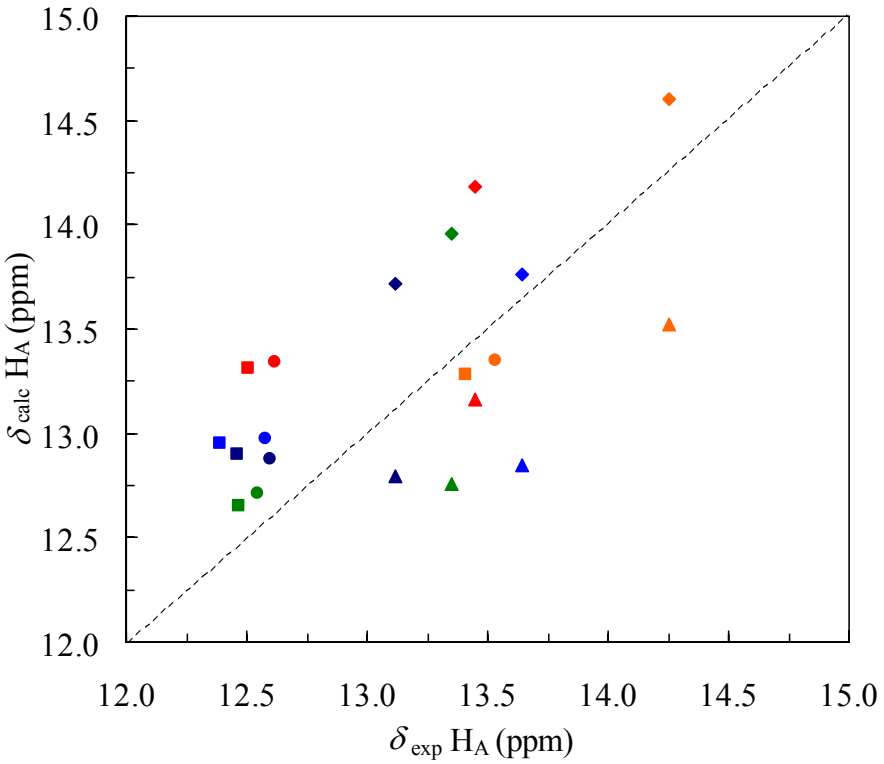

Fig. 7 Plot of calculated ^{1}H-NMR chemical shifts vs. experimentally observed ^{1}H-NMR chemical shifts of the H_A proton. The TSC, MTSC, *Z*-DMTSC, and *E*-DMTSC results are presented as squares, circles, diamonds, and triangles, respectively; the results for ANQ, I, MI, IS, and ALL series are in red, dark blue, blue, green, and orange, respectively.

4 Discussion

All investigated thiosemicarbazones have been studied having *Z* configuration for the C=N1′ bond. A focus of our study was to investigate the hydrogen bonding interaction between H_A and O_A, and only the Z configuration allows for this interaction. A more interesting feature of the geometry of these compounds is the structure around the N2′–C3′ bond. Figure 6 shows the two possible isomers obtained by rotation around this formal single bond, isomers that are labeled *Z* and *E* throughout the paper. We were interested in determining if both of these isomers can be formed (or can be present in solution) and whether they are actual conformers or structural isomers. The later is equivalent

to determining if the rotation around the N2′–C3′ bond were free or restricted. The rotation around the C3′–N4′ bond was investigated in a previous study of alloxan-based thiosemicarbazones [42] and is not investigated further here.

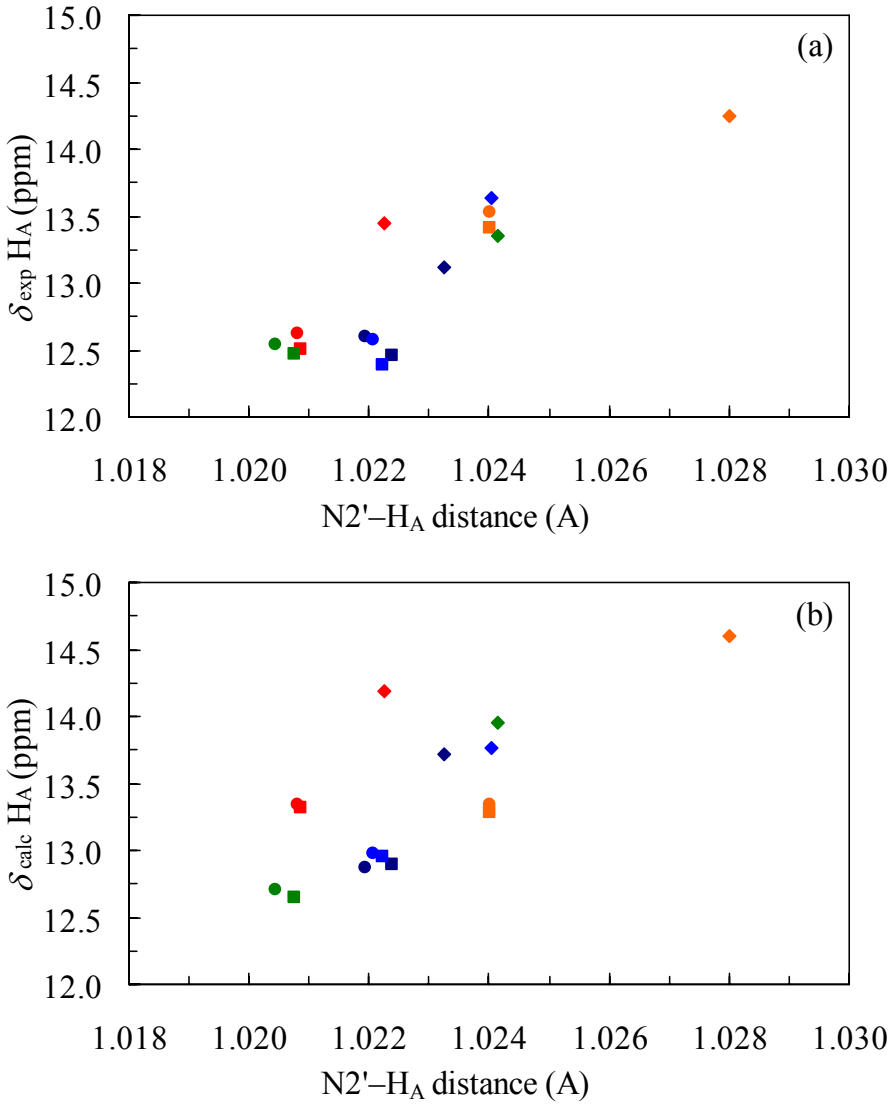

Fig. 8 Plots of experimental (a) and calculated (b) ^{1}H NMR chemical shift of H_A vs. the N2′–H_A internuclear distance.

While inspecting the optimized geometries obtained for both *E* and *Z* conformers of all 15 investigated thiosemicarbazones (Figures 1-5), it was found that all *E* isomers of TSC, all *E* isomers of MTSC and all *Z* isomers for MTSC have planar structures (i.e., C_s symmetry). The other isomers (all *Z* isomers of TSC, all *Z* and *E* isomers of DMTSC) are non-planar, mainly due to the hydrogen atoms or methyl groups bonded to N4′. For the *Z* isomers of TSC, H_B–N4′–C3′–N2′ and H_C–N4′–C3′–N2′ dihedral angles are about –10 and 5 degrees, respectively. For the *E* isomers of DMTSC, C_B–N4′–C3′–N2′ and C_C–N4′–C3′–N2′ dihedral angles are about 25 and 10 degrees, respectively, while for the *Z* isomers of DMTSC, C_B–N4′–C3′–N2′ and C_C–N4′–C3′–N2′ dihedral angles are about

10 and 5 degrees, respectively. The C_B represents the carbon atom of the methyl group replacing H_B, and the C_C represents the carbon atom of the methyl group replacing H_C.

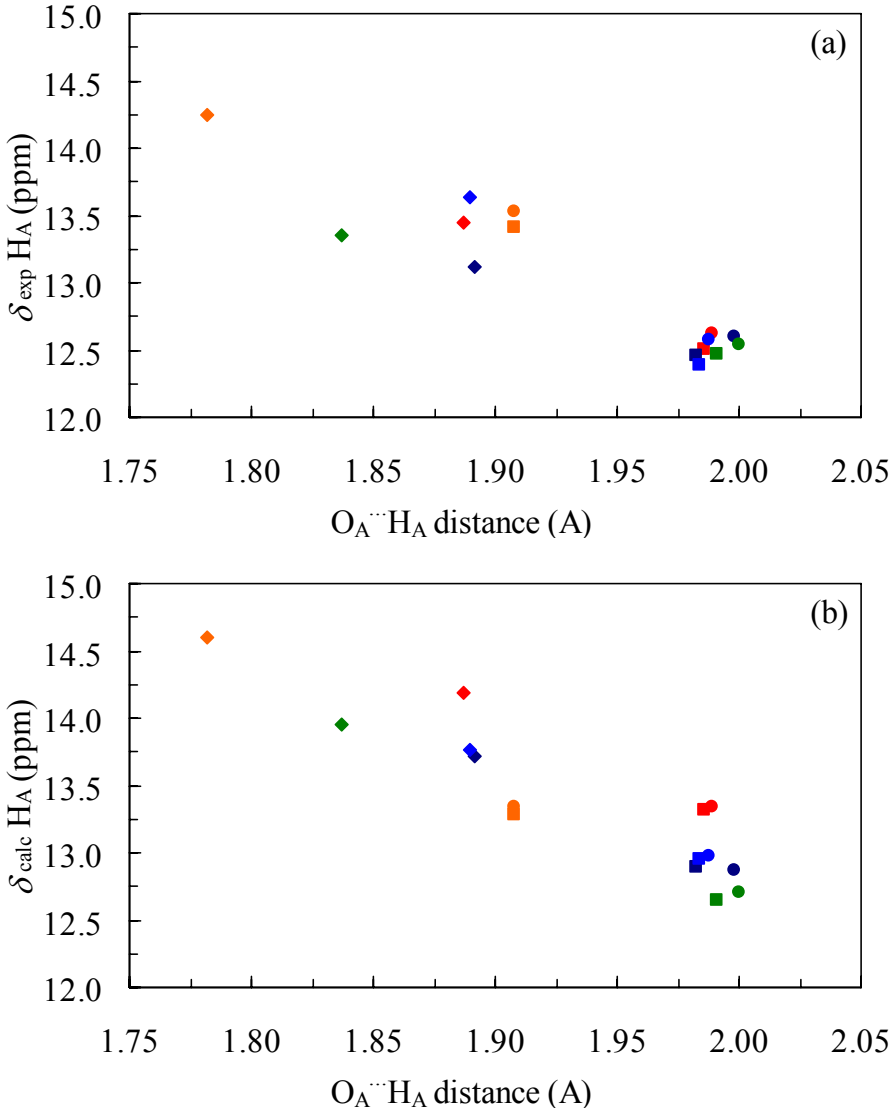

Fig. 9 Plots of experimental (a) and calculated (b) ^{1}H-NMR chemical shift of H_A vs. the O(4)···H_A internuclear distance.

It was also found that, even for the non-planar compounds, the N1′, N2′, H_A, S, C3′, and N4′ atoms are almost planar. This implies an sp^2 hybridization for N2′ and a partial double bond between N2′ and C3′, most likely a result of resonance with the C=S bond. A partial double bond between N2′ and C3′ will result in a shorter bond than a single C–N bond. The calculated N2′–C3′ bond distance is approximately 1.37–1.40 A in the optimized structures. This value is between the C–N bond distance of 1.46 A in CH_3–NH_2 and the C=N bond distance of 1.27 A in CH_2=NH, obtained at the same level of theory, mPW1PW91/6-31+G(p,d), as the TSC calculations. These results confirm the existence of a partial double bond between N2′ and C3′. Is this partial double bond strong enough

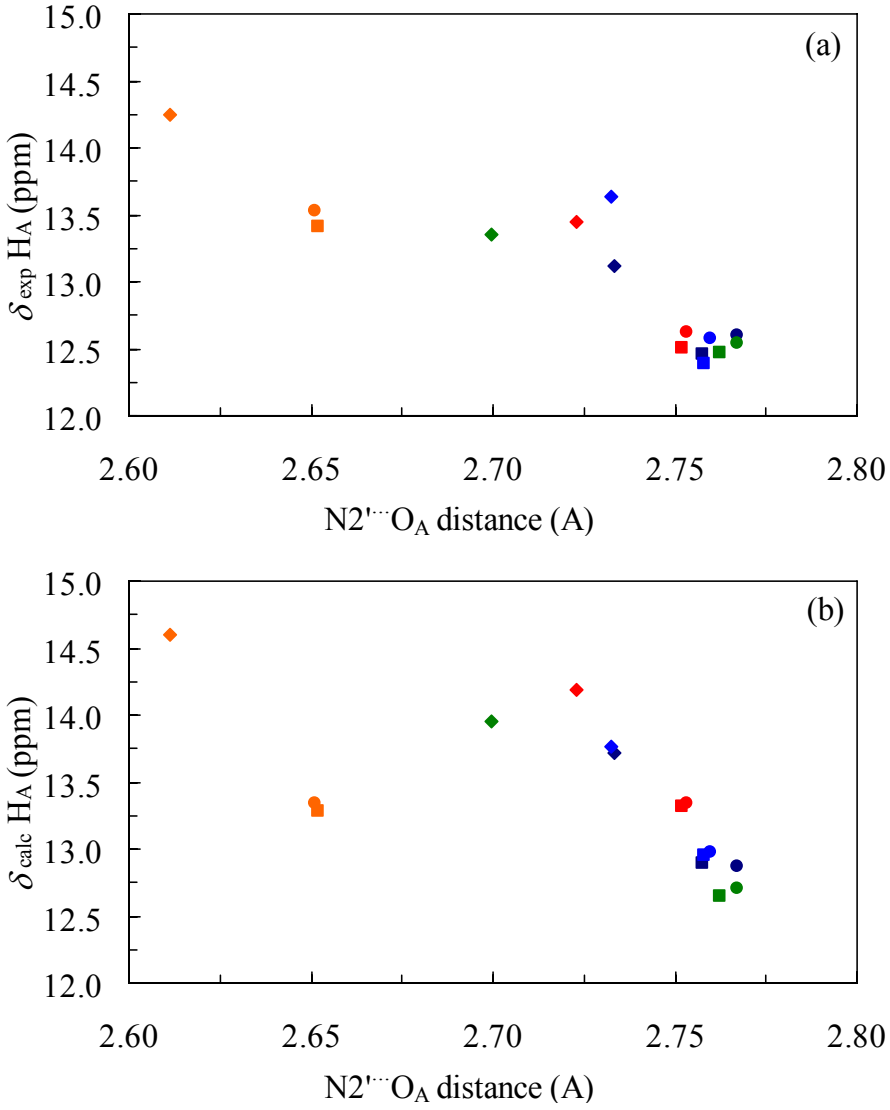

Fig. 10 Plots of experimental (a) and calculated (b) ^{1}H-NMR chemical shifts of H_A vs. the N2′···O(4) internuclear distance

to restrict the rotation around the N2′–C3′ bond?

The classical (i.e., zero-point exclusive) barrier heights for the $Z \rightarrow E$ isomerization process are calculated to be 9.16, 7.10, and 6.33 kcal/mol for I-TSC, I-MTSC, and I-DMTSC, respectively. For the reverse process, $E \rightarrow Z$, the calculated classical barrier heights are 16.37, 14.42, and 7.58 kcal/mol for I-TSC, I-MTSC, and I-DMTSC, respectively. These values are much larger than the barrier height for rotation around a single C–C bond (which is about 3 kcal/mol) supporting the idea of a restricted rotation along the N2′–C3′ bond, at least for I-TSC and I-MTSC. This restricted rotation along the N2′–C3′ bond suggests that the two isomers are structural isomers rather than conformers, and that the use of Z and E labels, which is consistent with the study of Bain et al. [24], is justifiable. The barrier height for I-DMTSC (as well as the ones for I-TSC and I-DMTSC) is probably underestimated by the level of theory used in this study consid-

ering that the calculated value would probably result in a relatively fast rotation on the NMR time scale in solution and therefore unique, averaged resonances for both isomers. The experimental observation of distinct resonances for each isomer suggests however, that the isomerization process, if at all possible, will be kinetically slow. The zero-point inclusive barrier heights for the $Z \rightarrow E$ isomerization process are also calculated to be high for a free rotation, with values of 9.13, 7.02, and 6.07 kcal/mol for I-TSC, I-MTSC, and I-DMTSC, respectively. The saddle points for the isomerization process have N1′–N2′–C3′–N4′ dihedral angles of approximately 108 degrees, and imaginary frequencies of around 91.7i, 58.7i, and 56.6i cm^{-1} for I-TSC, I-MTSC, and I-DMTSC, respectively. A complete description of the calculated saddle points is provided in the Supplementary Material [59].

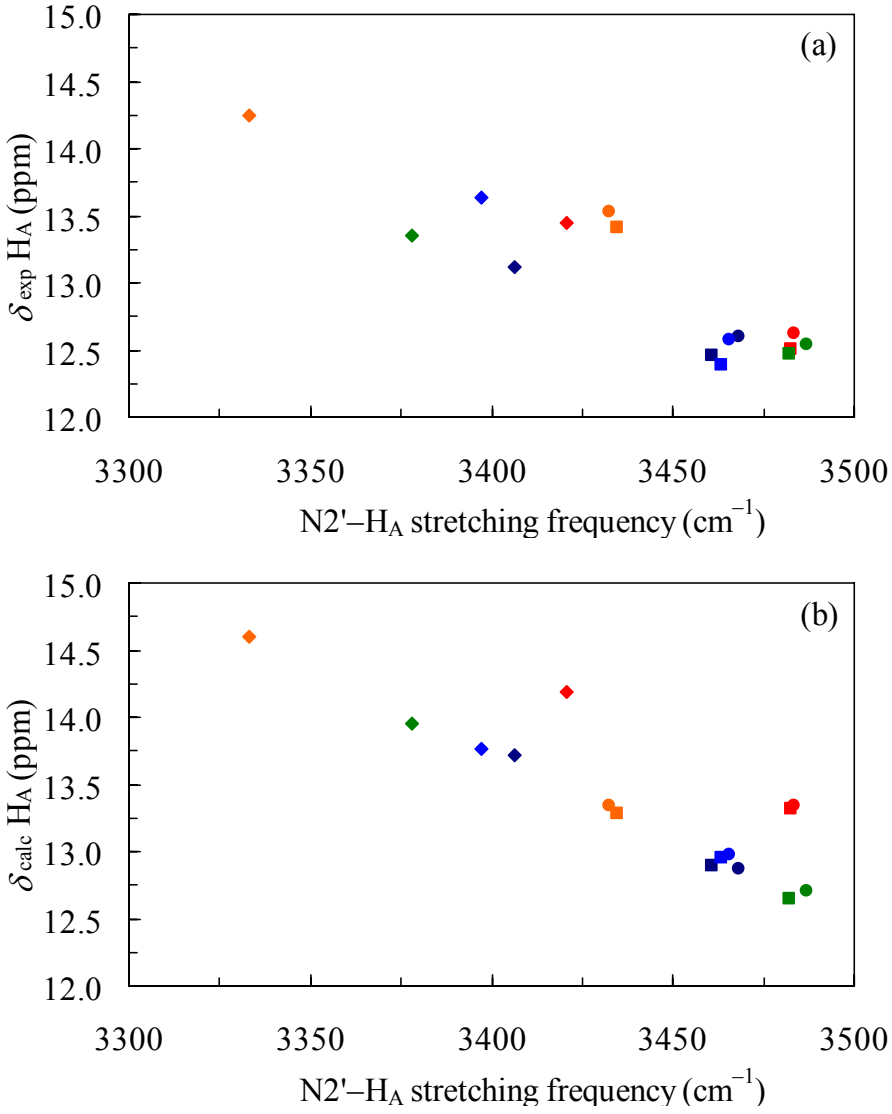

Fig. 11 Plot of calculated ^{1}H-NMR chemical shifts of H_A vs. calculated vibrational frequency for the N2′–H_A stretching

The energetics of the $Z \rightarrow E$ isomerization process have been investigated and the

calculated results are presented in Table 2. In this table, ΔE is the zero-point exclusive reaction energy, ΔH_0 is the enthalpy of reaction at 0 K (i.e., zero-point inclusive reaction energy), ΔH_{298} and ΔG_{298} are the enthalpy and the Gibbs free energy of reaction at 298 K. The results show that the $Z \rightarrow E$ process is exothermic for all investigated thiosemicarbazones. Also in Table 2, N_E/N_Z is the calculated relative distribution (based of the Gibbs free energy of the isomerization process) of the two isomers in the gas phase at 298 K. With one exception (I-DMTSC), the E isomer is calculated to always be more abundant than the Z isomer in the gas phase. It is also obvious that, for the TSC and MTSC compounds, the E isomer is much more abundant than the Z isomer (with an average of ΔG_{298} of –7.8 and –8.0 kcal/mol, respectively) while for DMTSC compounds the two isomers are much closer in stability. Based on these results, one can postulate that the presence of the Z isomers is very unlikely for the TSC and MTSC compounds, both in gas phase and in solution. Accordingly, in further investigating the chemical shifts and their correlation with various parameters, only the E isomers of TSC and MTSC are being considered. The results are, however, not so definitive for the DMTSC compounds, where both isomers are possible. Moreover, considering the solvation occurring in solution, the isomer with the higher dipole moment (the Z isomer for IS-DMTSC and ALL-DMTSC) will be preferred over the isomer with the smaller dipole moment. The dipole moments for the two isomers of each investigated thiosemicarbazone are listed in Table 2.

Besides investigating the structural aspects of the investigated compounds, another goal of this study is to gain a better understanding of the molecular properties determining the NMR behavior of these thiosemicarbazones. The main focus was on the ^{1}H NMR signals of the hydrazinic proton H_A because it appears at large chemical shifts (12.4 to 14.2 ppm), mainly due to strong hydrogen-bonding interaction with the carbonyl oxygen atom O_A. The calculated isotropic magnetic shielding tensors for the other protons are given in the Supplementary Material [59].

A plot of the calculated versus the experimental NMR chemical shifts for the H_A protons in all thiosemicarbazones (E isomers for TSC and MTSC, Z and E isomers for DMTSC) is represented in Figure 7. For each series of thiosemicarbazones, the chemical shift in TSC is smaller than that in MTSC. Experimentally, the chemical shift in DMTSC is larger than both TSC and MTSC. The calculated chemical shift values for the Z isomers of DMTSC show the same trend, while the chemical shifts for the E isomers are typically smaller than (or almost equal to) that of TSC and MTSC. The chemical shift difference between E and Z conformer of DMTSC compounds is approximately 1.00 ppm. Although the calculated chemical shift values are generally larger than the experimental ones, it is evident that a better correlation is obtained with the Z isomers of DMTSC (diamonds) rather than with the E isomers (triangles). This result implies that the Z isomer is more abundant in solution, and the experimental chemical shifts values for DMTSC are most likely obtained for the Z isomer. Accordingly, for the rest of our investigation, the E isomers of DMTSC were neglected, and only the Z isomers of DMTSC were considered.

The dependence of the H_A chemical shifts with various geometric parameters of the optimized structures was explored in more detail. Especially good linear relationships

with the N2′–H_A distance and the O_A···H_A distance were found. These dependencies are presented in Figures 8 and 9, respectively. The chemical shift of H_A appears further downfield as the N2′–H_A distance increases and the O_A···H_A distance decreases. These tendencies can be understood in terms of the hydrogen-bond interaction that exists between O_A and H_A. A stronger hydrogen-bond interaction will shorten the O_A···H_A distance, will elongate the N2′–H_A distance and will also causes a significant deshielding of the H_A proton leading to a further downfield NMR signal. There are also good correlations between the H_A chemical shifts and the N2′···O_A distance, as presented in Figure 10. In these correlations though, the alloxan-based thiosemicarbazones have a slightly different behavior and appear more as outliers. They, however, follow the same general trends of calculated H_A chemical shift decreasing with increasing the N2′···O_A distance. Based on these results, one can conclude that the local geometry near the H_A proton is a determining factor in its NMR properties.

If the chemical shifts were dependent on the N2′–H_A distance (due to the hydrogen bond between H_A and O_A), and considering that the internuclear distance is dependent on the strength of a chemical bond, then there should be a good correlation between the H_A chemical shift and the strength of the N2′–H_A bond. There is indeed a very good inverse relationship between the calculated frequency associated with the N2′–H_A stretching mode, a measure of the strength of the N2′–H_A bond, and the experimental and calculated H_A chemical shifts. These dependencies are presented in Figure 11. By investigating in more detail the dependencies in Figure 11, one can conclude that the force constant for the N2′–H_A stretching mode is different for the thiosemicarbazones in the ANQ series because they appear as outliers in the representations. A good linear correlation between the calculated or experimental chemical shifts of H_A and the calculated Mulliken charges or GAPT charges of H_A was not found. This is most likely due to the limitations of charge calculations that are known to be basis set dependent. Selected calculated Mulliken and GAPT charges are given in Table 5.

The calculations presented here allow for the identifications of the two isomers reported for I-DMTSC by West and coworkers [24]. In that study, West and coworkers reported two isomers for I-DMTSC in a ratio of 85:15. The methods used in that study did not allow for the complete identification of those isomers. The results presented here support the identification of the isomer with a greater chemical shift as the *Z* isomer, and the identification of the isomer with a lower chemical shift as the *E* isomer. This assignment is shown in Table 3. By making this assignment, however, the calculated ^{13}C NMR chemical shifts for C3′ (180.86 ppm for the *E* isomer and 175.80 for the *Z* isomer) are inconsistent with the experimental values (178.99 for the *E* isomer and 182.12 for the *Z* isomer). This disagreement could be a result of a possible misassignment of the experimental data [24]. Other calculated ^{13}C NMR chemical shifts as well as available experimental data are given in Table 4. These results as well as the values in the Supplementary Material [59] can be used to properly assign some NMR signals that are more difficult to assign based only on experiments.

5 Conclusions

This paper presents the results of a computational study at the mPW1PW91/6-31+G(d,p) level of theory of five series of thiosemicarbazones. We investigated various molecular properties including: the optimized structures, selected rotational barrier heights, dipole moments and ^{1}H and ^{13}C NMR chemical shifts. These results can be used as the basis for assigning experimentally observed NMR signals. Hydrogen-bond interactions are responsible for remarkable downfield ^{1}H NMR peaks for these types of compounds. The most important hydrogen-bond interaction for H_A is with O_A. Various linear relationships between the chemical shift of the hydrazinic proton H_A and selected geometric parameters or the N2′–H_A stretching frequency have been observed.

Acknowledgment

This research was partially supported by the College of Arts and Sciences and the Office of Research at Tennessee Technological University.

Supplementary Material

The Supplementary Material [59] includes geometries in Cartesian coordinates, calculated isotropic magnetic shielding tensors, Mulliken and GAPT atomic charges, energetic parameters, and frequencies for all structures optimized in this work.

References

[1] J.P. Scovill, D.L. Klayman and C.F. Franchino: "2-Acetylpyridine thiosemicarbazones. 4. Complexes with transition metals as antimalarial and antileukemic agents", *J. Med. Chem.*, Vol. 25, (1982), pp. 1261–1264.

[2] S. Padhye and G.B. Kauffman: "Transition metal complexes of semicarbazones and thiosemicarbazones", *Coord. Chem. Rev.*, Vol. 63, (1985), pp. 127–160.

[3] D.X. West, S.B. Padhye and P.B. Sonawane: "Structural and physical correlations in the biological properties of transition metal heterocyclic thiosemicarbazone and S-alkyl dithiocarbazate complexes", *Struct. Bonding*, Vol. 76, (1991), pp. 1–50.

[4] D.X. West, A.E. Liberta, S.B. Padhye, R.C. Chikate, P.B. Sonawane, A.S. Kumbhar and R.G. Yerande: "Thiosemicarbazone complexes of copper(II): structural and biological studies", *Coord. Chem. Rev.*, Vol. 123, (1993), pp. 49–71.

[5] T. Varadinova, D. Kovala-Demertzi, M. Rupelieva, M. Demertzis and P. Genova: "Antiviral activity of platinum (II) and palladium (II) complexes of pyridine-2-carbaldehyde thiosemicarbazone, *Acta Virol.*, Vol. 45, (2001), pp. 87–94.

[6] D. Kovala-Demertzi, M.A. Demertzis, J.R. Miller, C. Papadopoulou, C. Dodorou and G. Filousis: "Platinum(II) complexes with 2-acetylpyridine thiosemicarbazone. Syn-

thesis, crystal structure, spectral properties, antimicrobial and antitumour activity", *J. Inorg. Biochem.*, Vol. 86, (2001), pp. 555–563.

[7] A.R. Cowley, J.R. Dilworth, P.S. Donnelly, E. Labisbal and A. Sousa: "An Unusual Dimeric Structure of a Cu(I) Bis(thiosemicarbazone) Complex: Implications for the Mechanism of Hypoxic Selectivity of the Cu(II) Derivatives", *J. Am. Chem. Soc.*, Vol. 124, (2002), pp. 5270–5271.

[8] J.S. Lewis, D.W. McCarthy, T.J. McCarthy, Y. Fujibayashi and M.J. Welch: Evaluation of ^{64}Cu-ATSM in vitro and in vivo in a hypoxic tumor model, *J. Nucl. Med.*, Vol. 40, (1999), pp. 177–183.

[9] N. Takahashi, Y. Fujibayashi, Y. Yonekura, M.J. Welch, A. Waki, T. Tsuchida, N. Sadato, K. Sugimoto and H. Itoh: "Evaluation of ^{62}Cu labeled diacetyl-bis(N4-methylthiosemicarbazone) as a hypoxic tissue tracer in patients with lung cancer", *Ann. Nucl. Med.*, Vol. 14, (2000), pp. 323–328.

[10] ANQ-TSC = acenaphthene-1,2-dione 2-thiosemicarbazone, ANQ-MTSC = acenaphthene-1,2-dione 2-(N-methylthiosemicarbazone), ANQ-DMTSC = acenaphthene-1,2-dione 2-(N, N-dimethylthiosemicarbazone), I-TSC = 1H-indole-2,3-dione 3-thiosemicarbazone, I-MTSC = 1H-indole-2,3-dione 3-(N-methylthiosemicarbazone), I-DMTSC = 1H-indole-2,3-dione 3-(N, N-dimethylthiosemicarbazone), MI-TSC = 1-methylindole-2,3-dione 3-thiosemicarbazone, MI-MTSC = 1-methylindole-2,3-dione 3-(N-methylthiosemicarbazone), MI-DMTSC = 1-methylindole-2,3-dione 3-(N, N-dimethylthiosemicarbazone), IS-TSC = 1H-indole-2,3-dione-5-sulphonate 3-thiosemicarbazone, IS-MTSC = 1H-indole-2,3-dione-5-sulphonate 3-(N-methylthiosemicarbazone), IS-DMTSC = 1H-indole-2,3-dione-5-sulphonate 3-(N, N-dimethylthiosemicarbazone), ALL-TSC = pyrimidine-2,4,5,6(1H,3H)-tetrone 5-thiosemicarbazone, ALL-MTSC = pyrimidine-2,4,5,6(1H,3H)-tetrone 5-(N-methylthiosemicarbazone), ALL-DMTSC = pyrimidine-2,4,5,6(1H,3H)-tetrone 5-(N, N-dimethylthiosemicarbazone).

[11] J.W. Carter, R. Mayes, K.A. Pierce, R. Lawson and E.C. Lisic: "Structural determination of a series of ortho-quinone thiosemicarbazone compounds using NMR spectroscopy", *J. Und. Chem. Res.*, Vol. 2, (2003), pp. 73–77.

[12] T. Bell, R. Mayes, R. Lawson and E.C. Lisic: "Synthesis of a series of isatin-3-thiosemicarbazone-5-sulfonic acid compounds and structural characterization using NMR spectroscopy", *J. Und. Chem. Res.*, Vol. 3, (2004), pp. 39–45.

[13] H. Yamamoto, Y. Uchigata, H. Okamoto: "DNA strand breaks in pancreatic islets by in vivo administration of alloxan or streptozotocin", *Biochem. Biophys. Res. Commun.*, Vol. 103, (1981), pp. 1014–1020.

[14] H. Okamoto: "Molecular basis of experimental diabetes: degeneration, oncogenesis and regeneration of pancreatic B-cells of islets of Langerhans", *Bio Essays*, Vol. 2, (1985), pp. 15–21.

[15] N. Takasu, T. Asawa, I. Komiya, Y. Nagasawa and T. Yamada: "Alloxan-induced DNA strand breaks in pancreatic islets. Evidence for hydrogen peroxide as an inter-

mediate", *J. Biol. Chem.*, Vol. 266, (1991), pp. 2112–2114.
[16] J.D. Douros Jr., M. Brokl and A.F. Kerst (Gates Rubber Co.): US 3773952, 1973.
[17] E.C. Lisic, R.R. Nareddy, R. Huxford and E.C. Lisic: "Synthesis of a series of isatin-3-thiosemicarbazone-5-sulfonic acid compounds and structural characterization using NMR spectroscopy", *J. Und. Chem. Res.*, Vol. 5, (2006), pp. 61–66.
[18] S.N. Pandeya, S. Smitha, M. Jyoti and S.K. Sridhar: "Biological activities of isatin and its derivatives", *Acta Pharm.*, Vol. 55, (2005), pp. 27–46.
[19] D.J. Bauer: "Clinical experience with the antiviral drug marboran (1-methylisatin 3-thiosemicarbazone), *Ann. NY Acad. Sci.*, Vol. 130, (1965), pp. 110–117.
[20] D.J. Bauer: "The antiviral and synergistic actions of isatin thiosemicarbazone and certain phenoxypyrimidines in vaccinia infection in mice, *Br. J. Exp. Pathol.*, Vol. 36, (1955), pp. 105–114.
[21] P.W. Sadler: "Antiviral chemotherapy with isatin b-thiosemicarbazone and its derivatives, *Ann. NY Acad. Sci.*, Vol. 130, (1965), pp. 71–79.
[22] S.N. Pandeya and J.R. Dimmock: "Recent evaluations of thiosemicarbazones and semicarbazones and related compounds for antineoplastic and anticonvulsant activities, *Pharmazie*, Vol. 48, (1993), pp. 659–666.
[23] R.L. Thompson, S.A. Minton Jr., J.E. Officer and G.H. Hitchings: "Effect of heterocyclic and other thiosemicarbazones on vaccinia infection in the mouse, *J. Immunol.*, Vol. 70, (1953), pp. 229–234.
[24] G.A. Bain, D.X. West, J. Krejci, J. Valdes-Martinez, S. Hernandez-Ortega and R.A. Toscano: "Synthetic and spectroscopic investigations of N(4)-substituted isatin thiosemicarbazones and their copper(II) complexes, *Polyhedron*, Vol. 16, (1997), pp. 855–862.
[25] D.X. West, A.K. El-Sawaf and G.A. Bain: "Metal complexes of N(4)-substituted analogs of the antiviral drug methisazone {1-methylisatin thiosemicarbazone}, *Transit. Metal Chem.*, Vol. 23, (1998), pp. 1–6.
[26] D.J. Bauer and P. W. Sadler: "Structure-activity relations of the antiviral chemotherapeutic activity of isatin b-thiosemicarbazone, *Br. J. Pharmacol. and Chemoth.*, Vol. 15, (1960), pp. 101–110.
[27] H. Stuenzi: "Copper complexation by isatin b-thiosemicarbazones in aqueous solution, *Aust. J. Chem.*, Vol. 34, (1981), pp. 2549–2561.
[28] I. Chiyanzu, E. Hansell, J. Gut, P.J. Rosenthal, J.H. McKerrow and K. Chibale: "Synthesis and evaluation of isatins and thiosemicarbazone derivatives against cruzain, falcipain-2 and rhodesain, *Bioorg. Med. Chem. Lett.*, Vol. 13, (2003), pp. 3527–3530.
[29] I. Chiyanzu, C. Clarkson, P.J. Smith, J. Lehman, J. Gut, P.J. Rosenthal and K. Chibale: "Design, synthesis and anti-plasmodial evaluation in vitro of new 4-aminoquinoline isatin derivatives, *Bioorgan. Med. Chem.*, Vol. 13, (2005), pp. 3249–3261.
[30] M.C. Rodriguez-Arguelles, A. Sanchez, M.B. Ferrari, G.G. Fava, C. Pelizzi, G. Pelosi, R. Albertini, P. Lunghi and S. Pinelli: "Transition-metal complexes of isatin-

b-thiosemicarbazone. X-ray crystal structure of two nickel complexes, *J. Inorg. Biochem.*, Vol. 73, (1999), pp. 7–15.

[31] J.S. Casas, E.E. Castellano, M.S. Garcia Tasende, A. Sanchez and J. Sordo: "Reaction of dimethylthallium(III) acetate and isatin-3-thiosemicarbazone. Crystal and molecular structure of dimethyl(dimethylsulfoxide)(isatin-3-thiosemicarbazonato)thallium(III), *Inorg. Chim. Acta*, Vol. 304, (2000), pp. 283–287.

[32] N.T. Akinchan, P.M. Drozdzewski and W. Holzer: "Syntheses and spectroscopic studies on zinc(II) and mercury(II) complexes of isatin-3-thiosemicarbazone, *J. Mol. Struct.*, Vol. 641, (2002), pp. 17–22.

[33] M.B. Ferrari, C. Pelizzi, G. Pelosi and M.C. Rodriguez-Arguelles: "Preparation, characterization and X-ray structures of 1-methylisatin 3-thiosemicarbazone copper, nickel and cobalt complexes, *Polyhedron*, Vol. 21, (2002), pp. 2593–2599.

[34] T.S. Lobana, B.S. Sidhu, A. Castineiras, E. Bermejo and T. Nishioka: "Syntheses, NMR (1H, 31P) spectroscopy and crystal structures of complexes of copper(I) halides with isatin-3-thiosemicarbazone, *J. Coord. Chem.*, Vol. 58, (2005), pp. 803–809.

[35] H. Stuenzi: "Derivatives of isatin in aqueous solution. II. Z-E isomerism in isatin b-thiosemicarbazones, *Aust. J. Chem.*, Vol. 34, (1981), pp. 373–381.

[36] T.S. Rekha Lobana, R.J. Butcher, A. Castineiras, E. Bermejo and P.V. Bharatam: "Bonding Trends of Thiosemicarbazones in Mononuclear and Dinuclear Copper(I) Complexes: Syntheses, Structures, and Theoretical Aspects, *Inorg. Chem.*, Vol. 45, (2006), pp. 1535–1542.

[37] A.M.B. Bastos, A.F.D.C. Alcantara and H. Beraldo: "Structural analyses of 4-benzoylpyridine thiosemicarbazone using NMR techniques and theoretical calculations, *Tetrahedron*, Vol. 61, (2005), pp. 7045–7053.

[38] F.F. Jian, P.S. Zhao, Z.S. Bai and L. Zhang: "Quantum Chemical Calculation Studies on 4-Phenyl-1-(Propan-2-Ylidene)Thiosemicarbazide, *Struct. Chem.*, Vol. 16, (2005), pp. 635–639.

[39] C. Paiola, R. Cammi, P. Pelagatti and C. Pelizzi: "A density functional theory study of structural and NMR properties of SNN thiosemicarbazone ligands and their Pd(II) chlorocomplexes, *Theochem*, Vol. 623, (2003), pp. 105–119.

[40] H. Yuksek, I. Cakmak, S. Sadi, M. Alkan and H. Baykara: "Synthesis and GIAO NMR calculations for some novel 4-heteroarylidenamino-4,5-dihydro-1H-1,2,4-triazol-5-one derivatives: Comparison of theoretical and experimental 1H- and 13C-chemical shifts, *Int. J. Mol. Sci.*, Vol. 6, (2005), pp. 219–229.

[41] H. Yuksek, O. Guersoy, I. Cakmak and M. Alkan: "Synthesis and GIAO NMR calculations for some new 4,5-dihydro-1H-1,2,4-triazol-5-one derivatives: Comparison of theoretical and experimental 1H and 13C chemical shifts, *Magn. Reson. Chem.*, Vol. 43, (2005), pp. 585–587.

[42] N.W.S.V.N. DeSilva, E.C. Lisic and T.V. Albu: "Hybrid density functional theory investigation of a series of alloxan-based thiosemicarbazones and semicarbazones, *Central Eur. J. Chem.*, Vol. 4, (2006), pp. 646–665.

[43] C.C. Chambers, E.F. Archibond, S.M. Mazhari, A. Jabalameli, J.D. Zubkowski, R.H. Sullivan, E.J. Valente, C.J. Cramer and D.G. Truhlar: "Quantum chemical conformational analysis and x-ray structure of 4-methyl-3-thiosemicarbazide, *Theochem*, Vol. 388, (1996), pp. 161–167.

[44] C. Adamo and V. Barone: "Exchange functionals with improved long-range behavior and adiabatic connection methods without adjustable parameters: the mPW and mPW1PW models, *J. Chem. Phys.*, Vol. 108, (1998), pp. 664–675.

[45] J.P. Perdew, J.A. Chevary, S.H. Vosko, K.A. Jackson, M.R. Pederson, D.J. Singh and C. Fiolhais: "Atoms, molecules, solids, and surfaces: applications of the generalized gradient approximation for exchange and correlation, *Phys. Rev. B*, Vol. 46, (1992), pp. 6671–6687.

[46] K.B. Wiberg: "Comparison of density functional theory models' ability to reproduce experimental 13C-NMR shielding values, *J. Comp. Chem.*, Vol. 20, (1999), pp. 1299–1303.

[47] T.H. Sefzik, D. Turco, R.J. Iuliucci and J.C. Facelli: "Modeling NMR chemical shift: A survey of density functional theory approaches for calculating tensor properties, *J. Phys. Chem. A*, Vol. 109, (2005), pp. 1180–1187.

[48] H.F. Hameka: "Theory of magnetic properties of molecules, with particular emphasis on the hydrogen molecule, *Rev. Mod. Phys.* , Vol. 34, (1962), pp. 87–101.

[49] R. Ditchfield: "Self-consistent perturbation theory of diamagnetism. I. A gauge-invariant LCAO(linear combination of atomic orbitals) method for NMR chemical shifts, *Mol. Phys.*, Vol. 27, (1974), pp. 789–807.

[50] K. Wolinski, J.F. Hinton and P. Pulay: "Efficient implementation of the gauge-independent atomic orbital method for NMR chemical shift calculations, *J. Am. Chem. Soc.*, (1990), Vol. 112, pp. 8251–8260.

[51] R.S. Mulliken: "Electronic population analysis on LCAO-MO molecular wave functions. I, *J. Chem. Phys.*, Vol. 23, (1955), pp. 1833–1840.

[52] R.S. Mulliken: "Electronic population analysis on LCAO-MO molecular wave functions. II. Overlap populations, bond orders, and covalent bond energies, *J. Chem. Phys.*, Vol. 23, (1955), pp. 1841–1846.

[53] R.S. Mulliken: "Electronic population analysis on LCAO-MO molecular-wave functions. III. Effects of hybridization on overlap and gross AO populations, *J. Chem. Phys.*, Vol. 23, (1955), pp. 2338–2342.

[54] R.S. Mulliken: "Electronic population analysis on LCAO-MO molecular-wave functions. IV. Bonding and antibonding in LCAO and valence-bond theories, *J. Chem. Phys.*, Vol. 23, (1955), pp. 2343–2346.

[55] J. Cioslowski: "A new population analysis based on atomic polar tensors, *J. Am. Chem. Soc.*, Vol. 111, (1989), pp. 8333–8336.

[56] J. Cioslowski, T. Hamilton, G. Scuseria, B.A. Hess Jr., J. Hu, L.J. Schaad and M. Dupuis: "Application of the GAPT (generalized atomic polar tensor) population analysis to some organic molecules and transition structures, J. Am. Chem. Soc., Vol. 112, (1990), pp. 4183–4186.

[57] J. Cioslowski, P.J. Hay and J.P. Ritchie: "Charge distributions and effective atomic charges in transition-metal complexes using generalized atomic polar tensors and topological analysis, *J. Phys. Chem.*, Vol. 94, (1990), pp. 148–151.

[58] Gaussian 03, Revision B.02, M.J. Frisch, G.W. Trucks, H.B. Schlegel, G.E. Scuseria, M.A. Robb, J.R. Cheeseman, J. Montgomery, T. Vreven, K.N. Kudin, J.C. Burant, J.M. Millam, S.S. Iyengar, J. Tomasi, V. Barone, B. Mennucci, M. Cossi, G. Scalmani, N. Rega, G.A. Petersson, H. Nakatsuji, M. Hada, M. Ehara, K. Toyota, R. Fukuda, J. Hasegawa, M. Ishida, T. Nakajima, Y. Honda, O. Kitao, H. Nakai, M. Klene, X. Li, J.E. Knox, H.P. Hratchian, J. B. Cross, C. Adamo, J. Jaramillo, R. Gomperts, R.E. Stratmann, O. Yazyev, A.J. Austin, R. Cammi, C. Pomelli, J.W. Ochterski, P.Y. Ayala, K. Morokuma, G.A. Voth, P. Salvador, J.J. Dannenberg, V.G. Zakrzewski, S. Dapprich, A.D. Daniels, M.C. Strain, O. Farkas, D.K. Malick, A.D. Rabuck, K. Raghavachari, J.B. Foresman, J.V. Ortiz, Q. Cui, A.G. Baboul, S. Clifford, J. Cioslowski, B.B. Stefanov, G. Liu, A. Liashenko, P. Piskorz, I. Komaromi, R.L. Martin, D.J. Fox, T. Keith, M.A. Al-Laham, C.Y. Peng, A. Nanayakkara, M. Challacombe, P.M.W. Gill, B. Johnson, W. Chen, M.W. Wong, C. Gonzalez, J.A. Pople, Gaussian, Inc., Pittsburgh PA, 2003.

[59] The Supplementary Material includes geometries in Cartesian coordinates, calculated isotropic magnetic shielding tensors, Mulliken and GAPT atomic charges, energetic parameters, and frequencies for all structures optimized in this work. This material can be obtained from the corresponding author by emailing your request to albu@tntech.edu.